








Improving Landsat predictions of rangeland fractional cover with multitask learning and uncertainty

Brady W. Allred^{1,2}  | Brandon T. Bestelmeyer³ | Chad S. Boyd⁴ | Christopher Brown⁵ | Kirk W. Davies⁴  | Michael C. Duniway⁶  | Lisa M. Ellsworth⁷ | Tyler A. Erickson⁵  | Samuel D. Fuhlendorf⁸ | Timothy V. Griffiths⁹ | Vincent Jansen¹⁰ | Matthew O. Jones² | Jason Karl¹⁰ | Anna Knight⁶  | Jeremy D. Maestas¹¹ | Jonathan J. Maynard¹² | Sarah E. McCord³ | David E. Naugle¹ | Heath D. Starns¹³  | Dirac Twidwell¹⁴ | Daniel R. Uden^{14,15} 

¹W.A. Franke College of Forestry and Conservation, University of Montana, Missoula, MT, USA; ²Numerical Terradynamic Simulation Group, University of Montana, Missoula, MT, USA; ³Jornada Experimental Range, USDA Agricultural Research Service, Las Cruces, NM, USA; ⁴Eastern Oregon Agricultural Research Center, USDA Agricultural Research Service, Burns, OR, USA; ⁵Google, Inc, Mountain View, CA, USA; ⁶U.S. Geological Survey, Southwest Biological Science Center, Moab, UT, USA; ⁷Fisheries and Wildlife Department, Oregon State University, Corvallis, OR, USA; ⁸Natural Resource Ecology and Management, Oklahoma State University, Stillwater, OK, USA; ⁹USDA Natural Resources Conservation Service, Landscape Initiatives Team, Bozeman, MT, USA; ¹⁰Department of Forest, Rangeland, and Fire Sciences, University of Idaho, Moscow, ID, USA; ¹¹USDA Natural Resources Conservation Service, West National Technology Support Center, Portland, OR, USA; ¹²Sustainability Innovation Lab at Colorado, University of Colorado at Boulder, Boulder, CO, USA; ¹³Texas AgriLife Research, Texas A&M University, Sonora, TX, USA; ¹⁴Department of Agronomy and Horticulture, University of Nebraska–Lincoln, Lincoln, NE, USA and ¹⁵School of Natural Resources, University of Nebraska–Lincoln, Lincoln, NE, USA

Correspondence

Brady W. Allred

Email: brady.allred@umontana.edu

Handling Editor: Robert Freckleton

Abstract

1. Operational satellite remote sensing products are transforming rangeland management and science. Advancements in computation, data storage and processing have removed barriers that previously blocked or hindered the development and use of remote sensing products. When combined with local data and knowledge, remote sensing products can inform decision-making at multiple scales.
2. We used temporal convolutional networks to produce a fractional cover product that spans western United States rangelands. We trained the model with 52,012 on-the-ground vegetation plots to simultaneously predict fractional cover for annual forbs and grasses, perennial forbs and grasses, shrubs, trees, litter and bare ground. To assist interpretation and to provide a measure of prediction confidence, we also produced spatiotemporal-explicit, pixel-level estimates of uncertainty. We evaluated the model with 5,780 on-the-ground vegetation plots removed from the training data.
3. Model evaluation averaged 6.3% mean absolute error and 9.6% root mean squared error. Evaluation with additional datasets that were not part of the training dataset, and that varied in geographic range, method of collection, scope and size, revealed similar metrics. Model performance increased across all functional groups compared to the previously produced fractional product.

This is an open access article under the terms of the Creative Commons Attribution License, which permits use, distribution and reproduction in any medium, provided the original work is properly cited.

© 2021 The Authors. *Methods in Ecology and Evolution* published by John Wiley & Sons Ltd on behalf of British Ecological Society

4. The advancements achieved with the new rangeland fractional cover product expand the management toolbox with improved predictions of fractional cover and pixel-level uncertainty. The new product is available on the Rangeland Analysis Platform (<https://rangelands.app/>), an interactive web application that tracks rangeland vegetation through time. This product is intended to be used alongside local on-the-ground data, expert knowledge, land use history, scientific literature and other sources of information when making interpretations. When being used to inform decision-making, remotely sensed products should be evaluated and utilized according to the context of the decision and not be used in isolation.

KEYWORDS

conservation, convolutional neural network, grassland, machine learning, monitoring, rangeland management, remote sensing, temporal convolutional network

1 | INTRODUCTION

The ability to monitor rangeland vegetation and to quantify changes in cover with satellite remote sensing is revolutionary to the rangeland management discipline. Whereas on-the-ground data collection and monitoring is constrained logistically, satellite remote sensing scales easily, measuring the landscape across space and through time. Satellite measurements are modelled to predict rangeland indicators, providing key information for land managers and practitioners globally (Hill & Guerschman, 2020). Chief among these indicators is vegetation cover at species or functional group levels. Historically, cover was broadly categorical or thematic, and occurred at local, regional, or national levels (Homer et al., 2015). More recently, fractional cover is used to preserve the inherent complexity and heterogeneity of the landscape, estimating the proportion of an area covered by vegetation or land cover type (Xian et al., 2015). Fractional cover predictions, combined with local data and knowledge, can inform decision-making at multiple scales, providing land managers flexibility that is absent with categorical classifications and severely lacking with on-the-ground observations (Kennedy et al., 2014).

Fractional cover products are widely available for United States rangelands (Jones et al., 2018; Rigge et al., 2020; Zhang et al., 2019). To produce such products, on-the-ground data are correlated to remotely sensed measurements using regression tree approaches, with models developed and predictions performed individually for each desired component. Although robust, univariate regression trees do not capitalize on the ability to learn from shared representation among dependent variables. That is, relationships among functional groups are not learned and therefore may not be reflected in predictions. A learned multitask model, however, examines all output variables together and learns from inherent interactions and relationships present in the data, improving learning efficiency and prediction accuracy (Caruana, 1997). Variables that covary will be reflected in the model, for example, functional groups or species that are mutually exclusive or inversely related, such as tree and grass cover.

As these fractional cover products are the predictions of models, error and uncertainty are always present (Foody & Atkinson, 2003).

Prediction error is most commonly calculated as the difference between a single on-the-ground measurement and its predicted value, a calculation that can be done with certainty. Multiple errors can then be averaged to produce a generalized accuracy of the model, for example, root mean square error. Prediction uncertainty, however, differs from error in that it represents prediction confidence, or an expression of what is not known (Kendall & Gal, 2017). Consider the widely used example of a model that predicts whether an object in an image is a cat or dog, and is trained using only cat and dog data: if given cat or dog data, prediction confidence should be high; if given penguin data, prediction confidence should be low, as the model is unfamiliar with penguin data. While prediction error can only be calculated using individual on-the-ground measurements—and then averaged to obtain a generalized model accuracy—uncertainty can be calculated with every prediction, increasing its spatiotemporal utility. For the practitioner, uncertainty information can be used to assess prediction confidence, reliability, or use.

We describe a new rangeland fractional cover product that spans the western United States. We build upon previous advancements (Jones et al., 2018) by (a) utilizing a learned multitask approach to model the dynamic interactions of functional groups; and (b) generating pixel-level estimates of prediction uncertainty. We produce the fractional cover product annually from 1984 to 2019 at a moderate resolution of 30 m. It is made available for analysis, download and visualization through the Rangeland Analysis Platform (<https://rangelands.app/>) web application.

2 | MATERIALS AND METHODS

2.1 | Data

2.1.1 | Rangeland analysis platform—Fractional cover datasets

Jones et al. (2018) (hereafter referred to as fractional cover version 1.0) described the initial model and product released on the

Rangeland Analysis Platform in 2018. The new model and subsequent product described in this paper (hereafter referred to as fractional cover version 2.0) supersedes the initial version.

2.1.2 | Vegetation field data

We used 57,792 vegetation field data plots collected by the Bureau of Land Management Assessment, Inventory, and Monitoring and Landscape Monitoring Framework, and the Natural Resources Conservation Service National Resources Inventory programs (Nusser & Goebel, 1997; Toevs et al., 2011). Plots were collected from 2004 to 2019 (Table S1) across uncultivated, undeveloped, privately and publicly owned rangelands across 17 western US states. At each plot, vegetation was sampled using line point intercept methods on multiple transects. We followed methods outlined in Jones et al. (2018), using the 'first hit' to calculate cover and aggregating species into the following functional groups: annual forbs and grasses, perennial forbs and grasses, shrubs, trees, litter and bare ground. We randomly (stratified by state) divided the vegetation field data into training (90%, 52,012 field plots) and validation (10%, 5,780 field plots) datasets (Figure S1).

2.1.3 | Landsat imagery

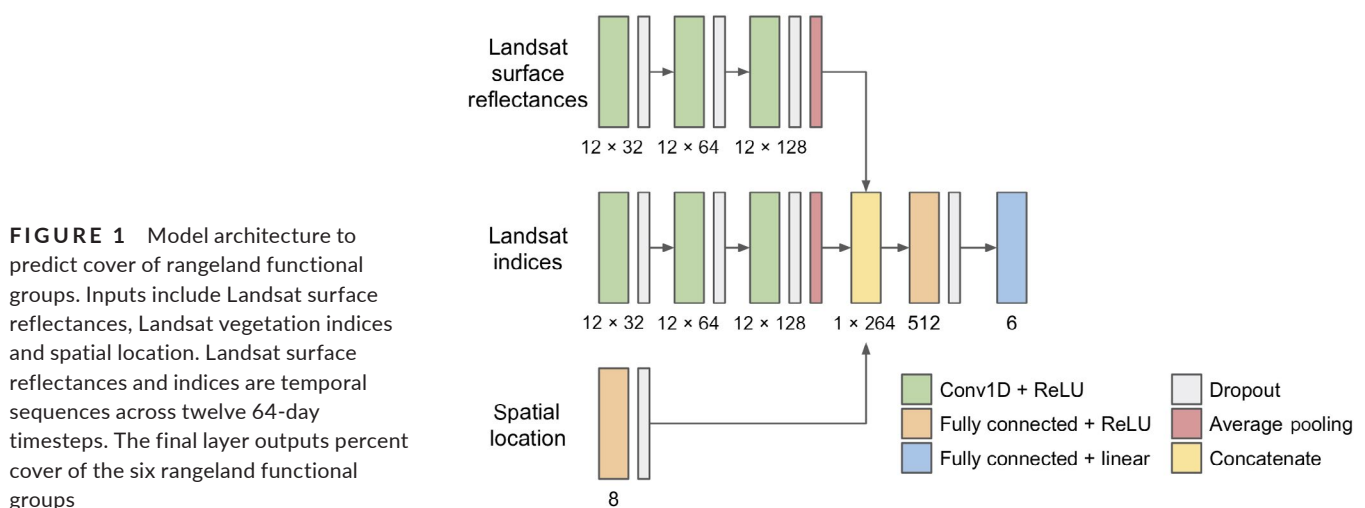
We used Landsat 5 TM, 7 ETM+ and 8 OLI surface reflectance products for predictors of fractional cover. We masked pixels identified as clouds, cloud shadow, snow and saturated surface reflectance. We divided the year into six, 64-day long timesteps (start dates occurring on day of year 001, 065, 129, 193, 257 and 321; the last timestep carried over into the following year) and calculated the average surface reflectance for visible, near infrared and shortwave bands (bands 1–5,7 for Landsat 5 TM and 7 ETM+; bands 2–7 for Landsat 8 OLI) in each timestep. We included both the six timesteps of the current year and the six timesteps of the previous year, resulting in 12 timesteps in total. To supplement surface reflectance measurements, we calculated

normalized difference vegetation index (NDVI) and normalized burn ratio two (NBR2) for each 64-day period. These indices represent vegetation characteristics that have been successful in modelling rangeland fractional cover (Jones et al., 2018). We reprojected and bilinearly resampled all Landsat imagery to a geographic coordinate system of approximately 30-m resolution.

2.2 | Model

We used Landsat surface reflectance measurements, vegetation indices and spatial location (XY coordinates) as covariates to predict rangeland fractional cover. The total number of covariates (10) was reduced significantly from fractional cover version 1.0. To generate a multivariate response, we used an artificial neural network to learn and predict cover for each functional group simultaneously. Artificial neural networks are mathematical algorithms that imitate the neurons found in mammalian brains and learn by considering examples (Goodfellow et al., 2016). For a review of artificial neural networks in ecology—specifically multilayered networks or deep learning—we refer the reader to Wäldchen and Mäder (2018) and Christin et al. (2019). We used a temporal convolutional network (i.e. one-dimensional convolution) as features associated with each vegetation field data plot varied sequentially through time, but not space. Temporal convolutions work well for satellite time-series classification (Pelletier et al., 2019; Zhong et al., 2019) and may also outperform standard recurrent neural networks such as long short-term memory (Bai et al., 2018).

We combined temporal convolutional layers with dropout, pooling and fully connected layers (Figure 1). Convolutional layers apply convolutions to the input; dropout layers randomly set input units to zero, a regularization technique to prevent overfitting; pooling layers reduce the size of representation, parameters and computation; and the fully connected layer connects to all units in the previous layer to produce the desired output. We used an Adam optimizer with a learning rate of 0.0001, a batch size of 32, a convolutional kernel width of three, and a dropout rate of 20%



(Srivastava et al., 2014); the number of filters increased from 32 to 128 over three layers, and the dilation rate increased from one to four. We utilized average pooling with a pooling size of 12 to reduce temporal sequences to a single value. We performed convolutions on Landsat surface reflectances and vegetation indices separately due to the differing characteristics they represent, concatenating layers prior to a fully connected layer (Figure 1). The final layer contained six units, corresponding to the six functional groups. To produce uncertainty estimates, we implemented dropout during prediction (Gal & Ghahramani, 2015), utilizing a 10% dropout rate before the fully connected layer. We repeated predictions four times, averaged results to obtain the predictive output, and calculated variance to estimate uncertainty.

We evaluated model performance by calculating mean absolute error (MAE), root mean square error (RMSE), residual standard error, (RSE) and the coefficient of determination (r^2) of the validation dataset. We compare evaluation metrics to fractional cover version 1.0. In addition to evaluation with the validation dataset, we also evaluated the model with datasets that were not part of the training process and that varied in geographic range, method of collection, scope and size (Table 1). We developed the model using the Keras library within Tensorflow and performed all image processing and predictions in Google Earth Engine (Gorelick et al., 2017) and Google Cloud AI Platform (AI Platform, 2020), respectively.

3 | RESULTS

3.1 | Model evaluation

Model results and evaluation metrics suggest strong relationships between predicted and on-the-ground measurements (Table 2 and Figure 2). Evaluation metrics of the validation dataset averaged 6.3 and 9.6% (MAE and RMSE, respectively) across rangeland functional groups. Residual standard errors of predicted and on-the-ground measurements varied from 4.6% to 12.7% among functional groups (Table 2). Coefficient of determination values ranged from 0.57 to 0.77 for most functional groups (Table 2). Evaluation metrics calculated with additional datasets that were not part of the training dataset also revealed similar metrics (Table 3). Model performance increased compared to fractional cover version 1.0 (Jones et al., 2018; Table 2), and is comparable to other US rangeland fractional products available over disparate geographies (Rigge et al., 2020; Zhang et al., 2019).

4 | DISCUSSION

We provide next generation predictions of annual, fractional cover of rangeland functional groups by implementing a multi-task learning approach across the western US (Figures 3 and 4).

TABLE 1 Additional datasets used in evaluation. These datasets varied in geographic range, method of collection, scope and size

Name	Location	Years	n	Description
Restore New Mexico Collaborative Monitoring Program (RestoreNM)	southwest New Mexico	2007–2017	788	Plots contained paired parallel 50-m transects 20 m apart. Transect-level cover used for evaluation
Sagebrush Steppe Treatment Evaluation Project (SageSTEP)	sagebrush steppe	2006–2014	227	Plots contained 15–24 subplots; five line transects in each subplot. Plot-level cover used for evaluation
Eastern Oregon Agricultural Research Center (EOARC)	eastern Oregon	2016	198	Plots contained three 20-m transects. Plot-level cover used for evaluation
USGS/NPS	Colorado Plateau	2007–2019	3,405	Plots contained two to three 50 m transects. Plot-level cover used for evaluation. See Supporting Information for more information
University of Idaho (UI)	central Idaho	2018–2019	60	Plots contained three 25-m transects. Plot-level cover used for evaluation

	Annual forb and grass	Perennial forb and grass	Shrub	Tree	Litter	Bare ground	Average
Fractional cover version 2.0 (this paper)							
MAE (%)	7.0	10.3	5.8	2.8	5.7	6.7	6.3
RMSE (%)	11.0	14.0	8.3	6.8	7.9	9.8	9.6
RSE (%)	8.8	12.7	6.6	5.9	4.6	7.9	—
r^2	0.58	0.77	0.57	0.65	0.37	0.73	—
Fractional cover version 1.0 (Jones et al., 2018)							
MAE (%)	7.8	11.1	6.9	4.7	—	7.3	7.56
RMSE (%)	11.8	14.9	9.9	8.5	—	10.6	11.14
RSE (%)	—	—	—	—	—	—	—
r^2 (%)	0.43	0.71	0.43	0.52	—	0.71	—

TABLE 2 Model evaluation metrics (mean absolute error, MAE; root mean square error, RMSE; residual standard error, RSE; and coefficient of determination, r^2) calculated using the respective validation dataset for fractional cover versions 1.0 and 2.0

FIGURE 2 Predictions of fractional cover relative to observed on-the-ground measurements ($n = 5,780$), separated by rangeland functional group. Diagonal dashed black line represents a 1:1 relationship; solid blue line is the linear fit between predicted and observed values. Coefficient of determination (r^2) and residual standard error (RSE) are reported in Table 2

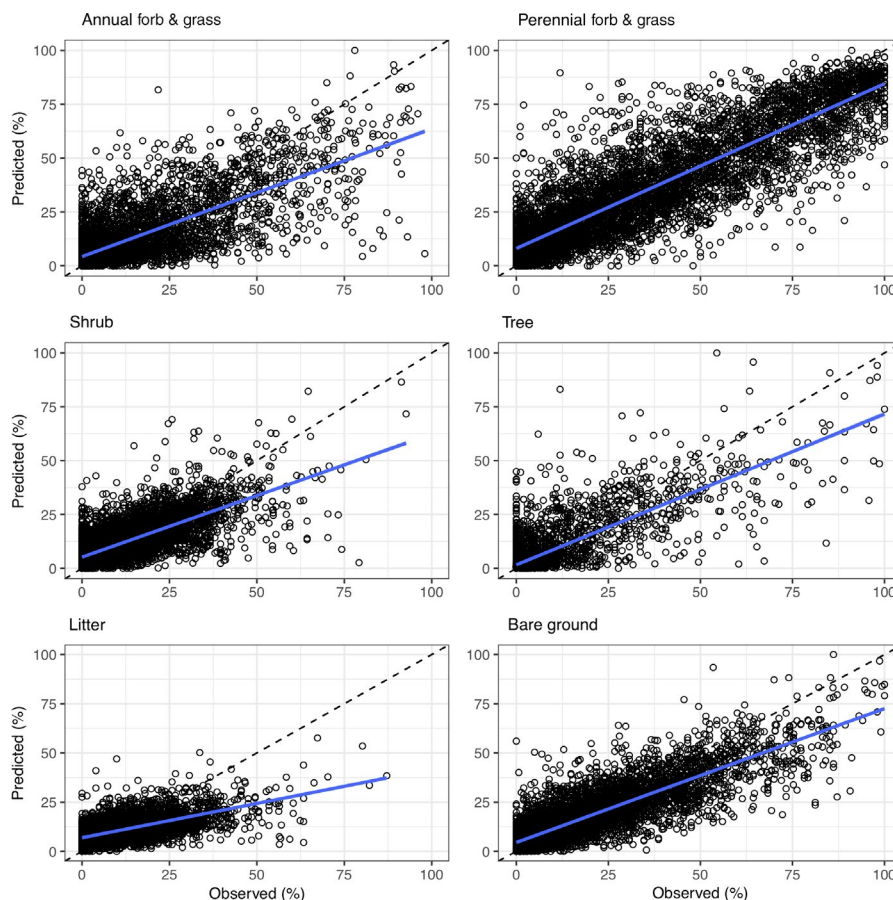


TABLE 3 Model evaluation metrics (mean absolute error, MAE; root mean square error, RMSE; and coefficient of determination, r^2) calculated using additional datasets described in Table 1

	Annual forb and grass	Perennial forb and grass	Shrub	Tree	Litter	Bare ground
RestoreNM						
MAE (%)	5.7	9.7	6.5	—	—	—
RMSE (%)	11.2	13.1	8.1	—	—	—
r^2	0.29	0.22	0.08	—	—	—
SageSTEP						
MAE (%)	9.0	13.2	8.3	—	—	8.9
RMSE (%)	13.3	18.1	9.8	—	—	11.8
r^2	0.19	0.25	0.27	—	—	0.49
EOARC						
MAE (%)	6.6	9.5	5.8	—	—	—
RMSE (%)	9.6	11.8	7.6	—	—	—
r^2	0.43	0.37	0.57	—	—	—
USGS/NPS						
MAE (%)	4.2	8.5	7.6	5.3	7.41	8.1
RMSE (%)	7.8	11.7	10.32	9.6	11.2	11.1
r^2	0.49	0.39	0.56	0.54	0.31	0.71
UI						
MAE (%)	8.0	10.5	9.8	—	—	3.2
RMSE (%)	10.6	13.3	12.1	—	—	4.3
r^2	0.56	0.28	0.30	—	—	0.31

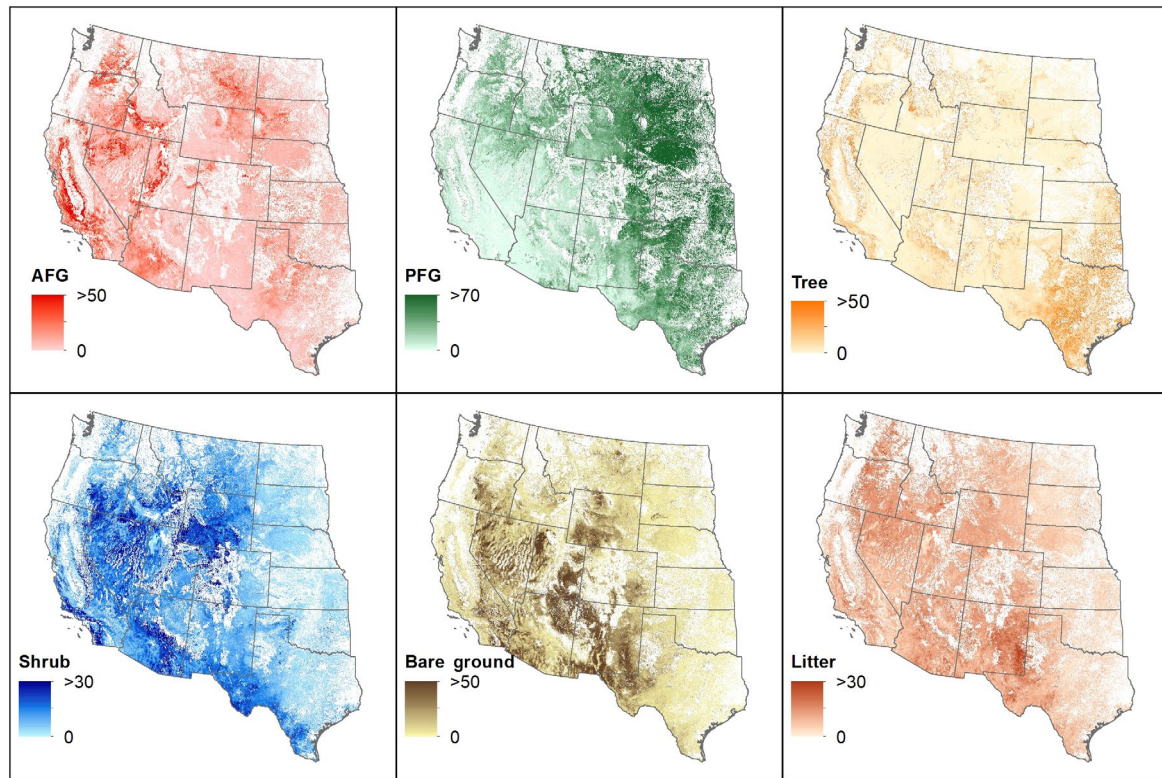


FIGURE 3 Fractional cover predictions of annual forbs and grasses (AFG), perennial forbs and grasses (PFG), shrubs, trees, litter and bare ground for 2019. White areas are non-rangeland as identified by Reeves and Mitchell (2011)

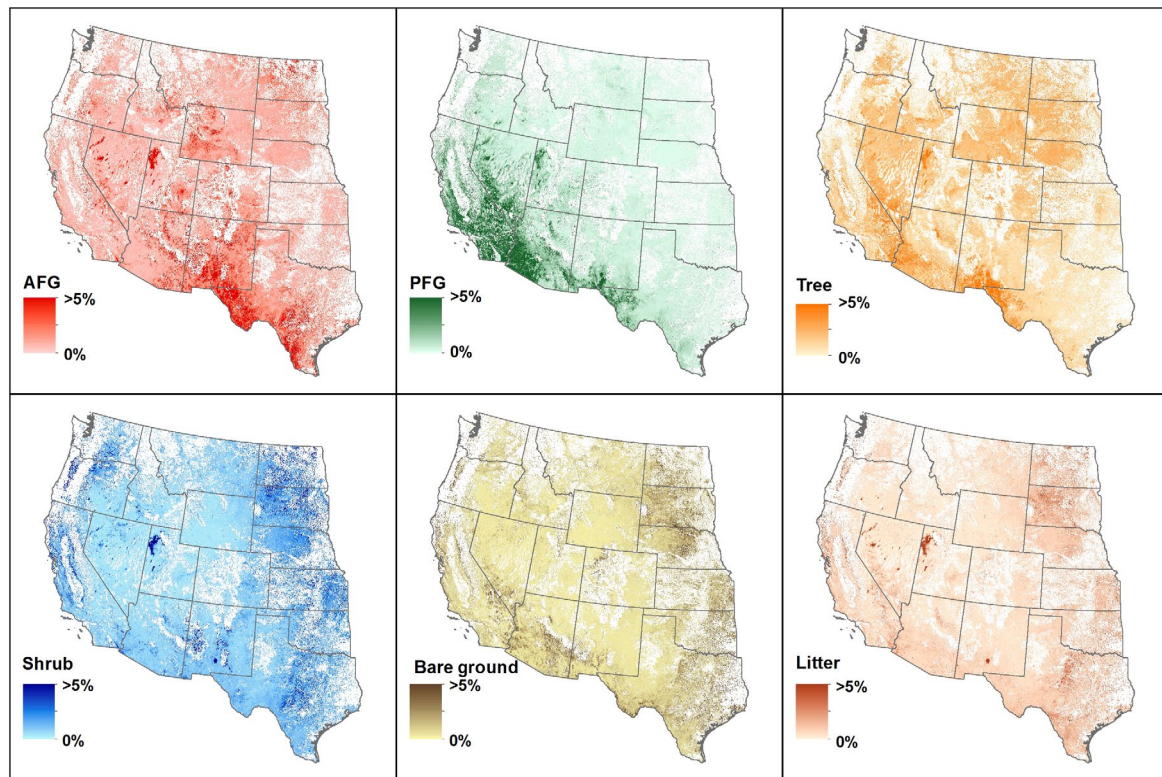


FIGURE 4 Fractional cover uncertainty of annual forbs and grasses (AFG), perennial forbs and grasses (PFG), shrubs, trees, litter and bare ground for 2019. White areas are non-rangeland as identified by Reeves and Mitchell (2011). Uncertainty was relativized to the fractional cover prediction

We improved upon our previous efforts (Jones et al., 2018) by (a) utilizing a neural network that models the dynamic interactions of functional groups; (b) reducing errors and improving model fit; and (c) providing spatiotemporal-explicit, pixel-level estimates of uncertainty alongside predictions. We deliver these data via the Rangeland Analysis Platform (<https://rangelands.app/>), an online and interactive web application that tracks rangeland vegetation through time.

The fractional cover of functional groups and cover types in rangelands reflect numerous ecosystem processes and ecosystem services. Changes in one functional group has predictable ecological impacts on other groups and the services they provide (Uden et al., 2019). For example, woody plant encroachment into grasslands constrains herbaceous grass cover and diminishes forage production and wildlife habitat (Archer et al., 2017), whereas annual grass invasion reduces perennial herbaceous plants and shrubs (Davies, 2008). While previous univariate modelling methods of fractional cover disregard this inherent covariation, a multitask model exploits it (Caruana, 1997). The underlying relationships among rangeland functional groups are learned and incorporated into the model, increasing accuracy (Figure 5). Although univariate predictions can be constrained or restricted post hoc to correct for or reduce such errors (Henderson et al., 2019), the goal of multitask learning is to learn and predict variables simultaneously. Furthermore, the shared representation of multitask learning

allows for covariance dynamics and interactions to be defined by the data, eliminating the need for predetermined conditions, rules, or thresholds.

When developing remotely sensed products, the goal is often to maximize model performance to increase accuracy. Error, however, is always present and should be understood and integrated into the application of that product and the decision being informed. Common model error metrics measure the average difference between predicted model output and individual on-the-ground measurements. This is generally calculated by withholding a portion (e.g. 5%–20%) of the model training dataset for validation (either entirely, or in a bootstrap aggregating approach). Error metrics therefore represent an average accuracy for the model given the validation dataset, but do not indicate any spatial or temporal variability of error. Attempts to visualize or aggregate errors across broad regions may appear helpful, but do little to characterize their spatial distribution or to help judge spatial accuracy (Jones et al., 2018; Zhang et al., 2019). Moreover, error is commonly calculated with only a minuscule fraction ($\ll 0.1\%$) of known measurements relative to total predictions, for example, the 5,780 known measurements used for validation (10% of the training dataset) in this exercise represents approximately $2e-8\%$ of total predictions.

The advantage of uncertainty information over error is its spatiotemporal utility: uncertainty is calculated with every prediction and therefore varies across space and time (Figure 6), while error

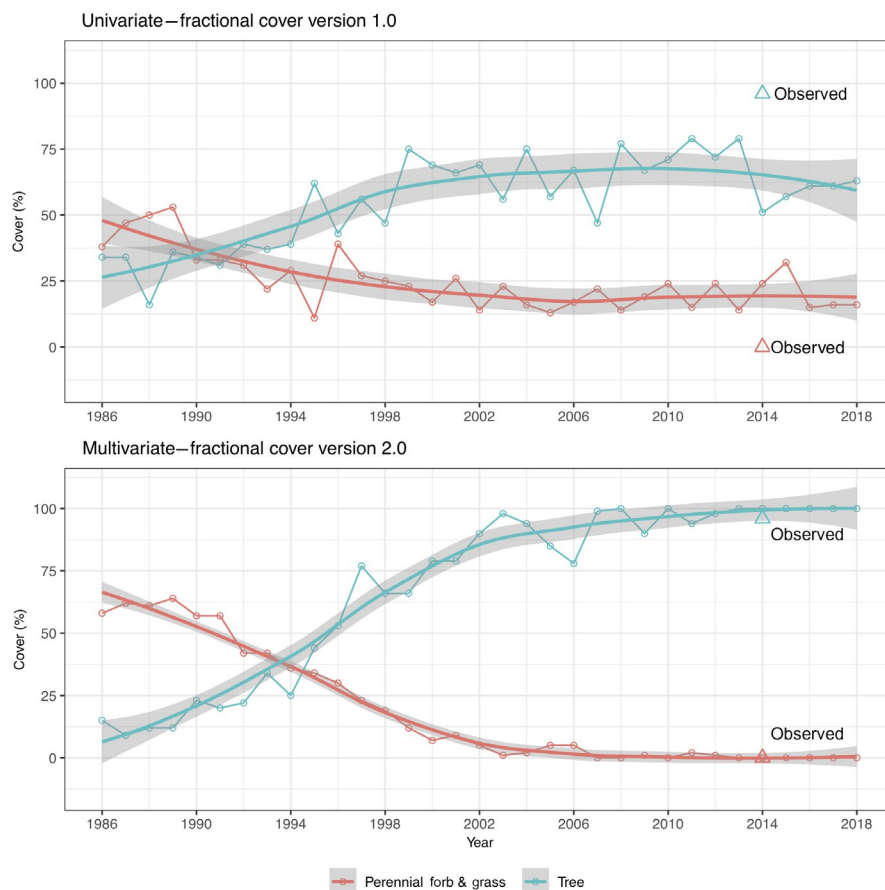


FIGURE 5 Univariate (top) and multivariate (bottom) predictions of perennial forb/grass and tree fractional cover for a single validation plot in an area with woody encroachment. Plot data were collected in 2014 and recorded 0% and 96% cover (triangular points) for perennial forb/grass and tree, respectively. Due to shared representation, multitask models and predictions better represent functional group dynamics. Fractional cover version 1.0 produced by Jones et al. (2018). Shaded lines represent locally estimated scatterplot smoothing

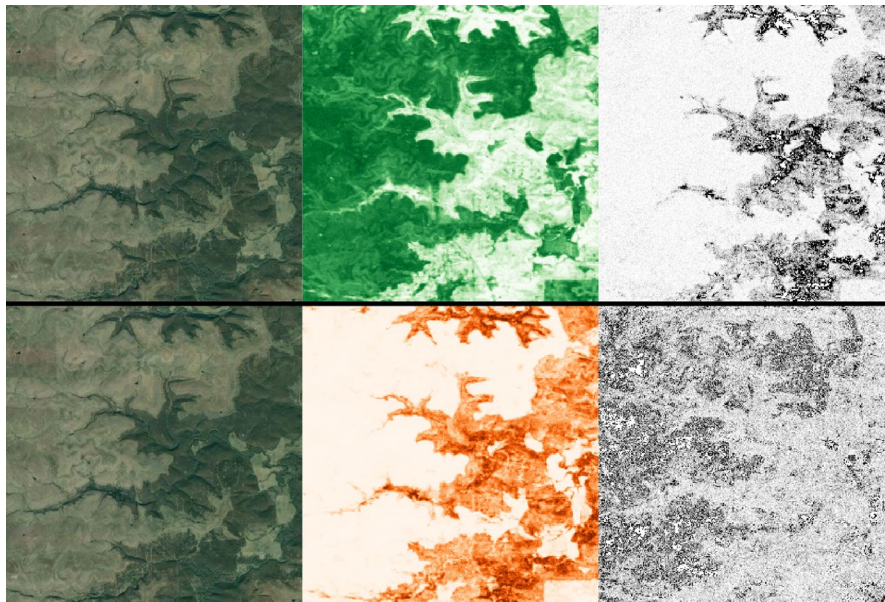


FIGURE 6 Aerial imagery (left), cover estimates (middle) and uncertainty estimates (right) for 2019 perennial forb and grass (top) and tree (bottom) functional group cover for a small region in the southern Great Plains. Light-to-dark values represent lower-to-higher values of cover and uncertainty. Greater uncertainty for perennial forb and grass estimates are present in areas dominated by trees and vice versa

does not (see discussion above). Uncertainty provides a measure of prediction confidence, that is, how reasonable is this prediction given the data used to build the model? If the characteristics of a location are generally represented within the model training data, uncertainty may be low and the corresponding prediction reasonable. If not as well represented within the model training data (e.g. areas such as high alpine, lava flows, arid playas), uncertainty may be high and the corresponding prediction unreasonable. Due to the fact that uncertainty is spatiotemporally explicit, it can be helpful in determining how to use model predictions on a case-by-case basis. For example, if uncertainty is high in a particular area or time period of interest, a practitioner can choose to gather additional local data or information, do a more detailed analysis, discuss with colleagues, etc. in order to expand decision inputs. Uncertainty can be integrated into the context of the decision being made for a particular place or time.

Operationalizing uncertainty information into decision-making presents new opportunities to learn about this type of information. While users often simply want to know if a prediction is 'right or wrong' or 'how far off it is', it is important to note that uncertainty does not provide this. Rather, uncertainty is a measure of model confidence (more specifically prediction variance), and should be thought about, processed and utilized in the same way that other confidence-, odds- or probability-type information is consumed, for example, precipitation probabilities supplied with weather forecasts. As such, there are no defined rules, standardized practices, thresholds, etc., to immediately employ when using uncertainty information. Use of such methods will vary depending upon the context of the decision being made. We recognize that it may be difficult to immediately incorporate uncertainty information into decision-making frameworks and workflows. We are confident, however, that with increased education, experience and exposure to these types of information, such barriers will be lessened and removed.

5 | CONCLUSIONS

Innovations in remotely sensed mapping of rangeland cover continue to present new opportunities to improve assessment, management and monitoring. We provide the latest advancement to expand the land management toolbox with improved predictions of fractional cover at a moderate resolution of 30 m, along with spatiotemporal-explicit uncertainty estimates, that can be used at such resolution or aggregated to broader scales. This product is intended to be used in combination with local on-the-ground data, expert knowledge, land use history, scientific literature and other sources of information when making interpretations. We emphasize that when being used to inform decision-making, remotely sensed products should be evaluated and utilized according to the context of the decision and not be used in isolation. Learning how to think about and use remotely sensed data, and suitably integrate them into decision frameworks and workflows, are next steps for improving the field of rangeland monitoring.

AUTHORS' CONTRIBUTIONS

B.W.A., M.O.J., J.D.M., D.E.N., T.V.G. and D.T. led the writing of the manuscript; B.W.A., C.S.B., T.A.E., M.O.J., J.D.M., S.E.M. and D.R.U. conceived, designed, implemented, or assisted with methodology; B.T.B., C.S.B., K.W.D., M.C.D., L.M.E., S.D.F., V.J., J.K., A.K. and H.D.S. collected, provided, or analysed data for additional evaluation. All authors contributed to drafts and gave final approval for publication. Any use of trade, product, or firm names is for descriptive purposes only and does not imply endorsement by the U.S. Government.

DATA AVAILABILITY STATEMENT

Data are available on the Rangeland Analysis Platform (<https://rangelands.app/>) and from <http://rangeland.nts.gov/data/rap/rap-vegetation-cover/>.

ORCID

- Brady W. Allred  <https://orcid.org/0000-0002-4017-8327>
- Kirk W. Davies  <https://orcid.org/0000-0002-5433-1396>
- Michael C. Duniway  <https://orcid.org/0000-0002-9643-2785>
- Tyler A. Erickson  <https://orcid.org/0000-0002-3597-1929>
- Anna Knight  <https://orcid.org/0000-0002-9455-2855>
- Heath D. Starns  <https://orcid.org/0000-0002-2501-3559>
- Daniel R. Uden  <https://orcid.org/0000-0003-3801-5489>

REFERENCES

- AI Platform. (2020). Retrieved from <https://cloud.google.com/ai-platform>
- Archer, S. R., Andersen, E. M., Predick, K. I., Schwinning, S., Steidl, R. J., & Woods, S. R. (2017). Woody plant encroachment: Causes and consequences. In D. D. Briske (Ed.), *Rangeland systems: Processes, management and challenges* (pp. 25–84). Springer International Publishing.
- Bai, S., Zico Kolter, J., & Koltun, V. (2018). An empirical evaluation of generic convolutional and recurrent networks for sequence modeling. *arXiv [cs.LG]*. Retrieved from <http://arxiv.org/abs/1803.01271>
- Caruana, R. (1997). Multitask learning. *Machine Learning*, 28(1), 41–75.
- Christin, S., Hervet, É., & Lecomte, N. (2019). Applications for deep learning in ecology. *Methods in Ecology and Evolution/British Ecological Society*, 10(10), 1632–1644. <https://doi.org/10.1111/2041-210X.13256>
- Davies, K. W. (2008). Medusahead dispersal and establishment in sagebrush steppe plant communities. *Rangeland Ecology & Management*, 61(1), 110–115. <https://doi.org/10.2111/07-041R2.1>
- Foody, G. M., & Atkinson, P. M. (2003). *Uncertainty in remote sensing and GIS*. John Wiley & Sons.
- Gal, Y., & Ghahramani, Z. (2015). Dropout as a Bayesian approximation: Representing model uncertainty in deep learning. *arXiv [stat.ML]*. Retrieved from <http://arxiv.org/abs/1506.02142>
- Goodfellow, I., Bengio, Y., Courville, A., & Bengio, Y. (2016). *Deep learning* (Vol. 1). MIT Press.
- Gorelick, N., Hancher, M., Dixon, M., Ilyushchenko, S., Thau, D., & Moore, R. (2017). Google Earth Engine: Planetary-scale geospatial analysis for everyone. *Remote Sensing of Environment*, 202, 18–27. <https://doi.org/10.1016/j.rse.2017.06.031>
- Henderson, E. B., Bell, D. M., & Gregory, M. J. (2019). Vegetation mapping to support greater sage-grouse habitat monitoring and management: Multi- or univariate approach? *Ecosphere*, 10(8), 361. <https://doi.org/10.1002/ecs2.2838>
- Hill, M. J., & Guerschman, J. P. (2020). The MODIS global vegetation fractional cover product 2001–2018: Characteristics of vegetation fractional cover in grasslands and savanna woodlands. *Remote Sensing*, 12(3), 406. <https://doi.org/10.3390/rs12030406>
- Homer, C., Dewitz, J., Yang, L., Jin, S., Danielson, P., Xian, G., Coulston, J. W., Herold, N., Wickham, J. D., & Megown, K. (2015). Completion of the 2011 National Land Cover Database for the conterminous United States—representing a decade of land cover change information. *Photogrammetric Engineering & Remote Sensing*, 81(5), 345–354.
- Jones, M. O., Allred, B. W., Naugle, D. E., Maestas, J. D., Donnelly, P., Metz, L. J., Karl, J., Smith, R., Bestelmeyer, B., Boyd, C., Kerby, J. D., & McIver, J. D. (2018). Innovation in rangeland monitoring: Annual, 30 m, plant functional type percent cover maps for U.S. rangelands, 1984–2017. *Ecosphere*, 9(9), e02430.
- Kendall, A., & Gal, Y. (2017). What uncertainties do we need in Bayesian deep learning for computer vision? In I. Guyon, U. V. Luxburg, S. Bengio, H. Wallach, R. Fergus, S. Vishwanathan, & R. Garnett (Eds.), *Advances in neural information processing systems* (Vol. 30, pp. 5574–5584). Curran Associates Inc.
- Kennedy, R. E., Andréfouët, S., Cohen, W. B., Gómez, C., Griffiths, P., Hais, M., Healey, S. P., Helmer, E. H., Hostert, P., Lyons, M. B., Meigs, G. W., Pflugmacher, D., Phinn, S. R., Powell, S. L., Scarth, P., Sen, S., Schroeder, T. A., Schneider, A., Sonnenschein, R., ... Zhu, Z. (2014). Bringing an ecological view of change to Landsat-based remote sensing. *Frontiers in Ecology and the Environment*, 12(6), 339–346. <https://doi.org/10.1890/130066>
- Nusser, S. M., & Goebel, J. J. (1997). The National Resources Inventory: A long-term multi-resource monitoring programme. *Environmental and Ecological Statistics*, 4(3), 181–204.
- Pelletier, C., Webb, G. I., & Petitjean, F. (2019). Temporal convolutional neural network for the classification of satellite image time series. *Remote Sensing*, 11(5), 523. <https://doi.org/10.3390/rs11050523>
- Reeves, M. C., & Mitchell, J. E. (2011). Extent of coterminous US rangelands: Quantifying implications of differing agency perspectives. *Rangeland Ecology & Management*, 64(6), 585–597. <https://doi.org/10.2111/REM-D-11-00035.1>
- Rigge, M., Homer, C., Cleaves, L., Meyer, D. K., Bunde, B., Shi, H., Xian, G., Schell, S., & Bobo, M. (2020). Quantifying western U.S. rangelands as fractional components with multi-resolution remote sensing and in situ data. *Remote Sensing*, 12(3), 412.
- Srivastava, N., Hinton, G., Krizhevsky, A., Sutskever, I., & Salakhutdinov, R. (2014). Dropout: A simple way to prevent neural networks from overfitting. *Journal of Machine Learning Research: JMLR*, 15(1), 1929–1958.
- Toevs, G. R., Karl, J. W., Taylor, J. J., Spurrier, C. S., Karl, M. S., Bobo, M. R., & Herrick, J. E. (2011). Consistent indicators and methods and a scalable sample design to meet assessment, inventory, and monitoring information needs across scales. *Rangelands*, 33(4), 14–20. <https://doi.org/10.2111/1551-501X-33.4.14>
- Uden, D. R., Twidwell, D., Allen, C. R., Jones, M. O., Naugle, D. E., Maestas, J. D., & Allred, B. W. (2019). Spatial imaging and screening for regime shifts. *Frontiers in Ecology and Evolution*, 7, 407. <https://doi.org/10.3389/fevo.2019.00407>
- Wäldchen, J., & Mäder, P. (2018). Machine learning for image based species identification. *Methods in Ecology and Evolution / British Ecological Society*, 9(11), 2216–2225. <https://doi.org/10.1111/2041-210X.13075>
- Xian, G., Homer, C., Rigge, M., Shi, H., & Meyer, D. (2015). Characterization of shrubland ecosystem components as continuous fields in the northwest United States. *Remote Sensing of Environment*, 168, 286–300. <https://doi.org/10.1016/j.rse.2015.07.014>
- Zhang, J., Okin, G. S., & Zhou, B. (2019). Assimilating optical satellite remote sensing images and field data to predict surface indicators in the Western U.S.: Assessing error in satellite predictions based on large geographical datasets with the use of machine learning. *Remote Sensing of Environment*, 233, 111382.
- Zhong, L., Hu, L., & Zhou, H. (2019). Deep learning based multi-temporal crop classification. *Remote Sensing of Environment*, 221, 430–443. <https://doi.org/10.1016/j.rse.2018.11.032>

SUPPORTING INFORMATION

Additional supporting information may be found online in the Supporting Information section.

How to cite this article: Allred BW, Bestelmeyer BT, Boyd CS, et al. Improving Landsat predictions of rangeland fractional cover with multitask learning and uncertainty. *Methods Ecol Evol*. 2021;12:841–849. <https://doi.org/10.1111/2041-210X.13564>